

Microstructure changes of the tungsten insert in CuCrZr compound electrode during resistance spot welding of galvanized sheets

Š. Emmer^{1,2*}, Z. Gábrišová¹, J. Kováčik³, P. Sejč¹, M. Lis⁴, J. Kulasa⁴

¹*Institute of Technologies and Materials, Faculty of Mechanical Engineering, Slovak University of Technology, Pionierska 15, 831 02 Bratislava, Slovak Republic*

²*Integrated Research of Materials and Applications STU, IVMA STU, Pionierska 15, 831 02 Bratislava, Slovak Republic*

³*Institute of Materials and Machine Mechanics, Slovak Academy of Sciences, Dúbravská cesta 9, 845 13 Bratislava, Slovak Republic*

⁴*Institute of Non-Ferrous Metals, ul. Sowińskiego 5, 44-100 Gliwice, Poland*

Received 18 May 2016, received in revised form 30 August 2016, accepted 4 September 2017

Abstract

The microstructures of the compound electrodes with tungsten insert were characterized using scanning electron microscopy. Resistance spot welding compound electrodes used in this study were prepared from precipitation-strengthened and cold-formed domed flat electrodes consisting of Cu-0.7Cr-0.2Zr alloy and tungsten insert. Detailed study of the microstructure of pure compound electrode, compound electrode after 800 cycles of mechanical compression load at room temperature and after 800 welds of the same sheets with protective coating were investigated using scanning electron microscope.

At room temperature, the cracks in the tungsten insert were observed. It was concluded that they originated from the technology of tungsten rods production. After welding, the microstructural results confirmed that Zn did not dissolve in tungsten. Unfortunately, the aluminium was found on the surface of the tungsten insert increasing the possibility to stamp the electrode to the welded sheet after 200 welds. The presence of aluminium is mostly in the form of aluminium oxides. However, the presence of Al-tungsten phases (WAl₄ and WAl₅) was not fully excluded. An important result is that it is necessary to address the problem of alumina, which, as was shown, affects the life of the studied compound electrode with tungsten insert.

Key words: resistance spot welding, compound electrode, tungsten insert, microstructure, life cycle

1. Introduction

The limiting factor in industrial manufacturing using resistance spot welding (RSW) is the life of the welding electrodes. Short life necessitates frequent electrode dressing or changing, resulting in lower production rates and higher costs. Also, weld quality is more variable towards the end of the life of an electrode, particularly when welding coated steels [1, 2]. Electrode deterioration causes the growth of the electrode tip diameter, which has been shown to be dominant in determining the deterioration in weld quality [3].

The basic problem during the RSW of galvanized sheets is, in addition to the weldability of the sheets themselves, the contamination of the working surface of the welding electrode by zinc or Zn-based alloy, which is used for corrosion protection of sheet metal. Contamination of the working surface of the electrode with zinc leads to changes in its structure, resulting in a change in its mechanical and physical properties. In the case of Cu-based (CuCr, CuCrZr alloys) electrodes, the most common brass phases occur as a result of Zn reaction with used copper alloy [4, 5], thus leading to the formation of new structural phases that have, for example, lower hardness, lower melting

*Corresponding author: e-mail address: stefan.emmer@stuba.sk

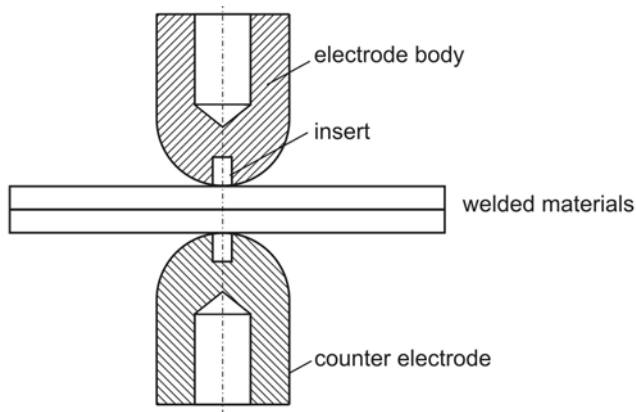


Fig. 1. Compound CuCrZr electrodes with a tungsten insert in welding position.

point, lower electrical conductivity, etc., when compared with the properties of original electrode material. These structural changes adversely affect the life cycle of the electrode for the RSW. In mass production, for example in the automotive industry during the welding of galvanized sheets of car bodies, the life of welding electrodes is significantly limiting factor. The short life of the electrode very often requires dressing or replacing the electrode which results in a reduction of the production speed and an increase in production costs.

The problem of electrode life for RSW was studied very often and is described in many papers [1–6]. Basically, there are several ways to increase the life of electrodes for RSW of galvanized sheets: cleaning of the electrodes between welding, changing of welding parameters after certain number of cycles, creation of compound electrodes with various inserts, coating of the surface of the electrodes by PVD, CVD, galvanization and electro-spark deposition [6–9].

As was mentioned above one option is the preparation of compound electrodes. Since tungsten shows no affinity to molten zinc, compound electrodes with tungsten inserts of various size and shape were developed during last decades. However, no systematic study of the microstructure of such compound electrodes during RSW has been done. Therefore, this study aims to analyse the structural and mechanical changes induced in the compound electrode with the cylindrical tungsten insert during welding of galvanized sheets.

2. Materials and experimental procedure

Resistance spot welding (RSW) compound electrodes used in this study were prepared from precipitation-strengthened and cold-formed domed flat electrodes consisting of a Cu-Cr-Zr alloy (Cu-0.7Cr-0.2Zr) [10]. The electrode has a dome shape with a working

area of 3.6 mm. The electrode of Class II precipitation hardened Cu-Cr-Zr alloys is common electrode very often used for RSW of zinc plated galvanized steels. A tungsten insert of cylindrical shape with a diameter of 2.4 mm was stamped into the centre of the work surface to create compound electrode (see Fig. 1).

The tungsten insert was chosen on the basis of the appropriate physical properties of tungsten for this application. These features include: no reaction with zinc; molten zinc does not wet tungsten; the high melting temperature of tungsten; its refractory properties; high resistance to flow also at elevated temperatures [11].

To investigate the microstructure changes of the tungsten insert in CuCrZr compound electrode during resistance spot welding (RSW) of galvanized sheets, the following material for welding was chosen: Sheets HX 220 BD-Z100 MBO 0.8 mm thick. It is high-strength structural steel (EN 10 346) with zinc coatings (100 g m^{-2} , two-sided).

HX 220 BD steel composition is as follows: C 0.1 wt.%, Si 0.5 wt.%, Mn 0.7 wt.%, P max. 0.06 wt.%, S max. 0.025 wt.%, Nb 0.09 wt.%, Ti 0.12 wt.%, Fe balanced. The composition of zinc coating consists almost entirely of zinc (> 99 %) and is lead free. The composition determined by SEM shows also presence of aluminium 1.18 at.%, oxygen 1.63 at.%, and 97.19 at.% is zinc.

The mechanical loading (without electric current) and also welding were carried out by ARO welding pliers, type: XMA, with permanent power $S_p = 26 \text{ kVA}$. The pliers were of the “C” type with the direct movement of the upper (testing) electrode. Welding parameters were set up using a ULB control system with a fully controllable welding process parameters system. The welding force was set to a constant value of $F = 2.2 \text{ kN}$. The current passing time was also set to a constant value of 10 periods (0.2 s).

Because the degradation processes of the electrode during resistance spot welding are induced by the simultaneous action of the mechanical stress and temperature, the microstructural changes on the compound electrode were observed and evaluated at two different stages:

(i) after 800 cycles of mechanical loading at room temperature with an applied force up to $F = 2.2 \text{ kN}$ in the identical state as for welding;

(ii) after 800 welds made using the welding parameters listed in Table 1.

The microstructures of the compound electrode with tungsten insert were characterized using scanning electron microscopy (SEM), JEOL IT 300 with EDS analyser. The analyses were focused on structural changes in the compound electrode, i.e., on Cu-CrZr matrix and the tungsten insert after 800 cycles of mechanical loading at room temperature, and after 800 welds.

Table 1. Working parameters of resistance spot welding process

Applied force, F (kN)	2.2
Welding time, t (s)	0.2 ($\pm 10\%$)
Welding current, I (kA)	5.16–6.07
Welding voltage, U (V)	1.00

3. Results and discussion

3.1. The initial state of the compound electrode tip

The initial state of the tip of the compound electrode before the realization of the experiments is in Fig. 2. Obviously, after the pressing of the tungsten

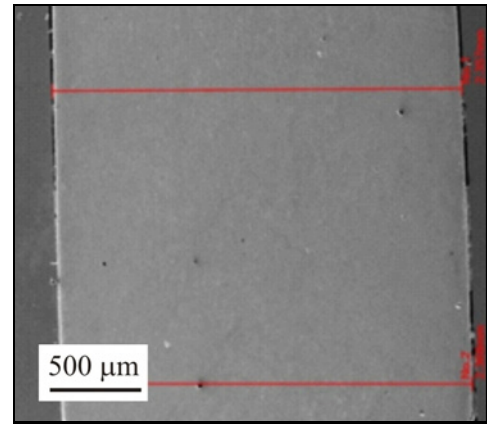


Fig. 2. Tungsten insert in CuCrZr matrix initial state.

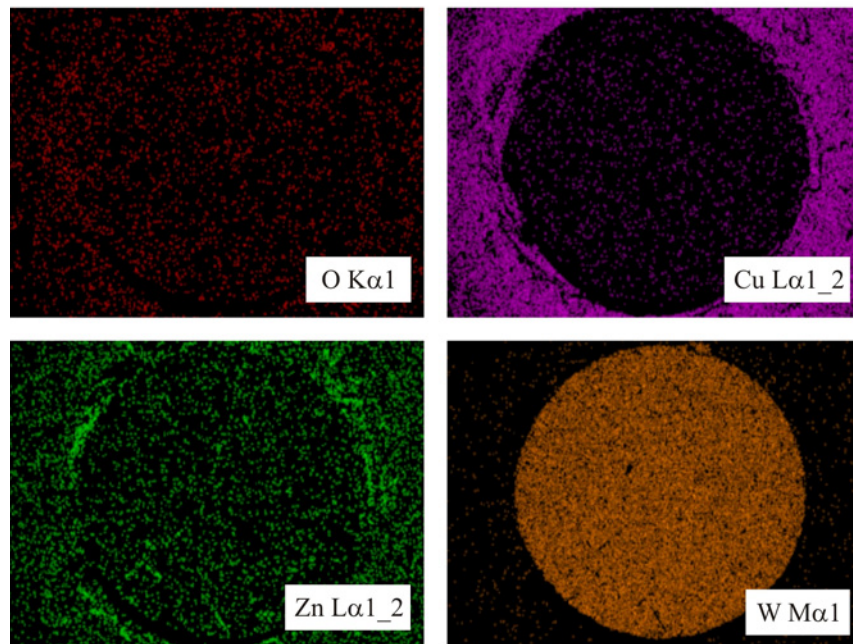
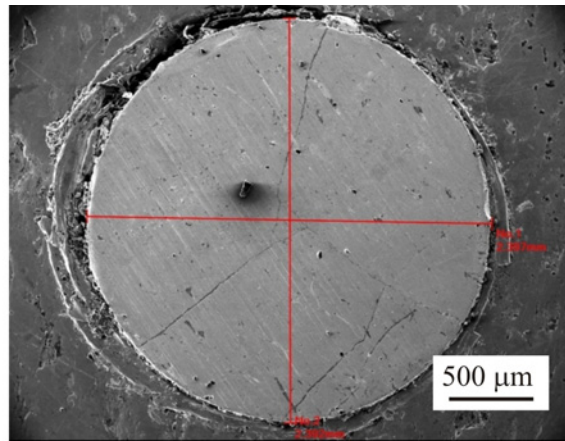


Fig. 3. The surface of tungsten insert in CuCrZr matrix and EDS maps of compound electrode tip after 800 cycles of mechanical loading up to 2.2 kN.

wire with a diameter of 2.4 mm into the CuCrZr matrix, no deformation of the tungsten insert, or the surrounding CuCrZr electrode matrix is identified. There are no cracks in the insert, even no microcracks. Only mechanical attachment of the tungsten insert in the matrix having a defined sharp interface can be observed. Besides that, there are some air gaps in certain regions of the insert-matrix interface.

3.2. The compound electrode tip after 800 cycles of mechanical loading up to 2.2 kN

On the surface of the tip of the compound electrode, the presence of cracks in the tungsten insert can be observed after 800 cycles of mechanical loading up to 2.2 kN (see Fig. 3). The measured diameters of the tungsten insert in two perpendicular directions are 2.392 mm and 2.397 mm. It implies that there is almost no change when compared to the diameter of the insert measured before the mechanical loading of the compound electrode.

At the boundary between the insert and CuCrZr matrix, it is possible to observe the discontinuous filling of the gap with steel coating material (as later discussed ESD analysis showed), respectively with its oxides. These are mechanically pressed into the gap that is present after the tungsten insert is pressed into the CuCrZr matrix of the compound electrode.

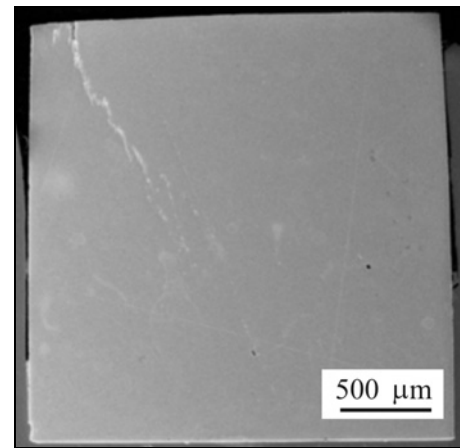


Fig. 4. Tungsten insert in CuCrZr matrix after 800 cycles of mechanical loading up to 2.2 kN.

As Fig. 4 documents, the surface cracks spread from the electrode surface during mechanical loading. From the surface cracks at the front of the tungsten insert, the cracks spread into the volume of tungsten insert. In addition to this, variations in the size of the interface between the tungsten insert and the CuCrZr matrix can be observed: near the tip of the compound electrode, the gaps are relatively large and clearly visible. Their size was considerably increased by mechani-

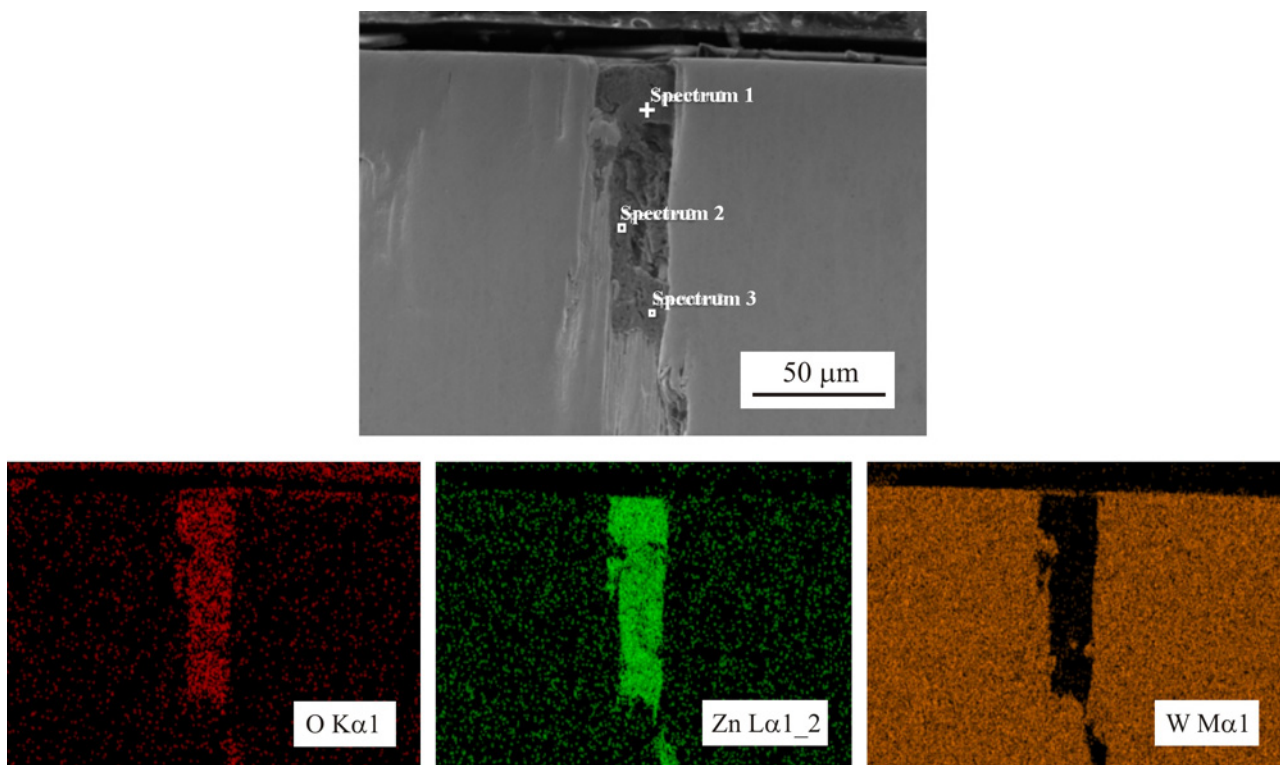


Fig. 5. SEM of crack in tungsten insert at the tip surface of the compound electrode and corresponding EDS maps (compound electrode tip after 800 cycles of mechanical loading up to 2.2 kN).

Table 2. Average EDS map results at Spectra 1–3 at crack in tungsten insert at the tip surface of compound electrode after 800 cycles of mechanical loading up to 2.2 kN

Element	Line type	(at.%)
O	K series	48.1 ± 2.0
Zn	L series	51.9 ± 2.0
Total		100.0

cal pressing of material mentioned above originating from the Zn-based coating on galvanized steel sheet metal. At the lower part of the tungsten insert around its periphery, it is also possible to observe the compressed material of CuCrZr matrix.

Origin of these cracks can be connected to cohesive adherence of tungsten blank which was produced via cold pressing followed by hot rotating forging and subsequent drawing to the desired rod size. These intermediate surfaces in tungsten rods increased oxide content, which caused the creation of cracks in tungsten insert of the compound electrode during mechanical loading at room temperature.

SEM-EDS map analysis of the tip of the compound electrode (see Fig. 3) showed the presence of the products of plastic deformation that were created during the subsequent cyclic loading of the compound electrode with a compressive force of 2.2 kN. In particular, there are the basic materials of which the composite electrode is created (tungsten insert and CuCrZr matrix – only Cu map is provided for simplification) and new products that were generated during cyclic loading. These new products can be found mostly in the gap between the insert and the CuCrZr matrix. As confirmed by SEM investigation of the cross-section of tungsten insert, these products are also present in the frontal cracks of tungsten insert (Fig. 5). Point spectral EDS analysis confirmed that ZnO phase was created (Fig. 5 and Table 2). ZnO comes from the protective passivation layer of the Zn coating on the steel sheet. However, most probably also oxidation of zinc took place during 800 cycles of mechanical loading in compression.

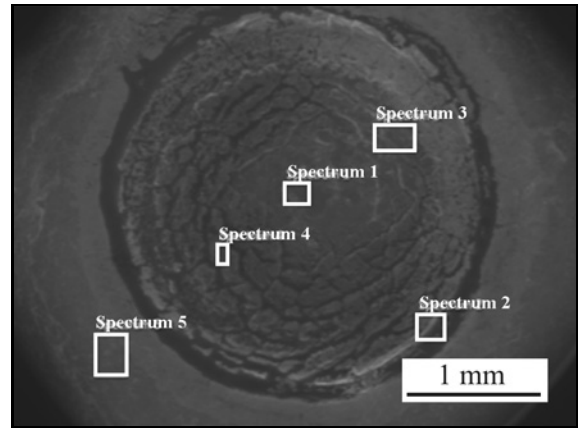


Fig. 6. EDS area analysis of compound electrode tip after 800 welds.

3.3. The compound electrode tip after 800 welds

Figure 6 shows a tip surface of a compound electrode consisting of tungsten insert and CuCrZr matrix. It is observed that the gap between insert and matrix is filled with products of thermo-mechanical loading of the electrode tip. ESD analyses showed that the front surface of the insert besides Zn also contains Al (Table 3). It is clear that the presence of Al or phases containing Al is due to thermo-mechanical loading of the tip of the compound electrode on the welded material. The presence of zinc and aluminium on the surface in the case of CuCrZr electrodes has been studied in several works [1, 7]. Zn effect on reducing the lifetime of CuCrZr electrodes is mainly in the formation of electron alloy (brass) which negatively affects the life of the electrode. Al effect on reducing the lifetime of CuCrZr electrodes is mainly in the formation of Cu-Al alloy which also negatively affects the life of the electrode [12]. In the case of a compound electrode, besides zinc on the front of the tungsten, Al phase was also identified. This significantly alters the degradation processes that occur in the case of tungsten insert of compound electrodes. Representative frontal surface ESD spectra are shown in Fig. 7 and show the presence of Al on the front surface of the tungsten insert.

Table 3. EDS area results at Spectra 1, 2 and 4 at compound electrode tip after 800 welds

Spectrum	Element	(wt.%)	Spectrum	Element	(wt.%)	Spectrum	Element	(wt.%)
1	Al	31.7	2	W	63.6	4	Al	38.5
	O	22.7		Zn	19.9		O	21.2
	Zn	17.7		Al	7.8		Zn	12.8
	Fe	16.0		Fe	6.1		W	11.1
	W	6.4					Fe	6.7

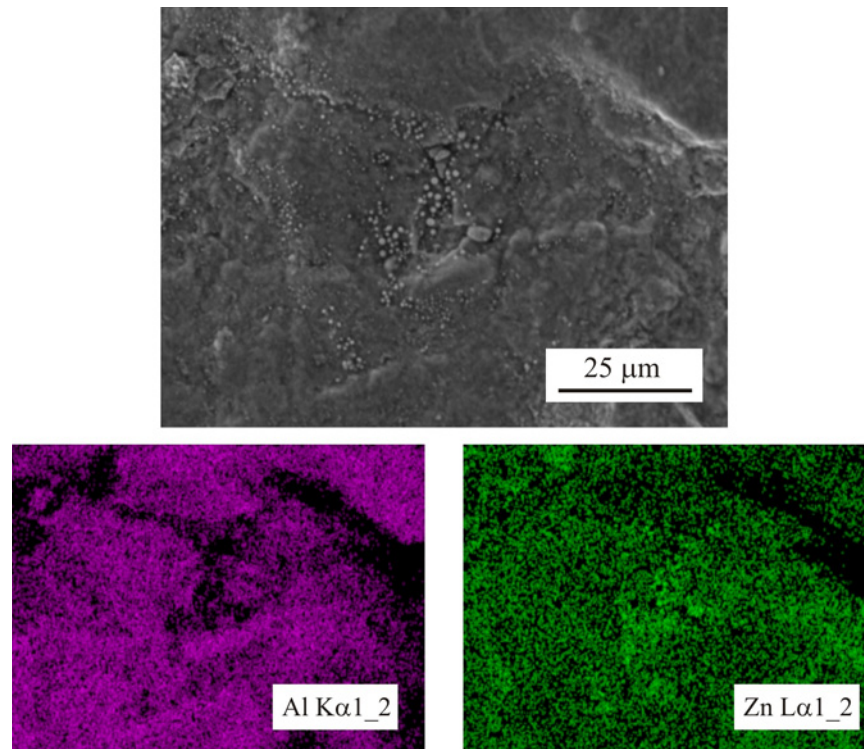


Fig. 7. Detailed EDS maps of compound electrode tip after 800 welds.

Table 4. EDS point analysis results at Spectra 6 and 9 on tungsten insert surface of compound electrode after 800 welds

Spectrum	Element	(wt.%)	Spectrum	Element	(wt.%)
6	Zn	96.7	9	Al	61.9
	Fe	1.4		O	12.5
	Al	1.1		Zn	10.2
	C	0.2		Fe	9.9

A detailed analysis of the elements present on the forehead of tungsten insert (Spectra 1, 2 and 4) has shown that Al is present predominantly in the central part of the tungsten insert. Zn is located in the central part and also around the circumference of the tungsten insert. Further spectral analysis showed that Zn was present on the front surface of tungsten insert in the form of spherical particles (Figs. 7 and 8) and Al in the form of layers (Fig. 7). This was confirmed by spectral point analysis of Zn particles, see, e.g., Spectrum 6 in Fig. 8 and Table 4.

Figure 9 shows a cross-section of the compound electrode with tungsten insert after 800 welds. The macroscopic analysis confirms that cracks in the tungsten insert from the tip of the compound electrode are expanded deep into the volume of tungsten insert. Furthermore, a significant plastic deformation of the insert outer face can be observed: The original diameter

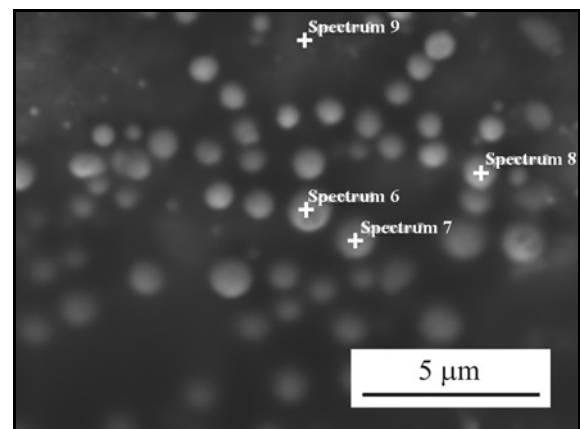


Fig. 8 Detailed EDS point analysis (at high zoom) of compound electrode tip after 800 welds.

of 2.4 mm increased to the diameter of 2.64 mm. It is also possible to observe on the perimeter of tungsten insert a new phase which is continuously connected to the surface of the compound electrode (1.926 and 2.096 mm length concerning the tip of compound electrode – Fig. 9). The deformation of the insert and the formation of continuous phase along the insert circumference is due to the cyclic thermal stress in the electrode.

Moreover, the openings of the cracks at the insert surface are also filled with continuous phases (see

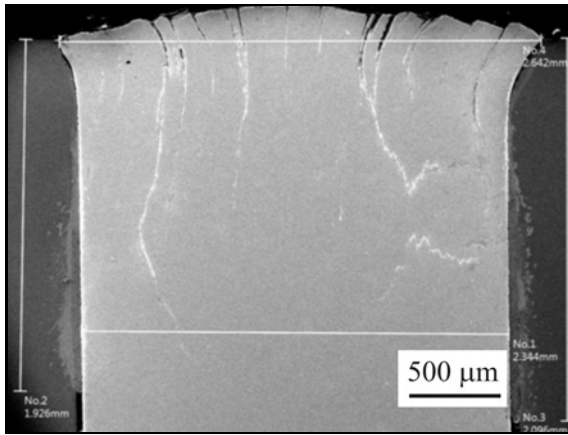


Fig. 9. Tungsten insert in CuCrZr after 800 welds.

Table 5. EDS maps results of the cross-section of the tungsten insert in compound electrode tip after 800 welds

Element	Line type	(at.%)
O	K series	37.44
Al	K series	4.61
Zn	L series	14.18
Tungsten	M series	43.76
Total:		100.00

Fig. 10). Map analysis suggests that these phases are similar to the phases observed on the front of the tung-

sten insert of the compound electrode (Table 5). When compared to pure mechanical stress without applied current, the occurrence of Al in cracks of tungsten insert was observed in addition to Zn phase. On the other hand, the occurrence of Al is mainly correlated to the surface of the compound electrode tip. Zn phase

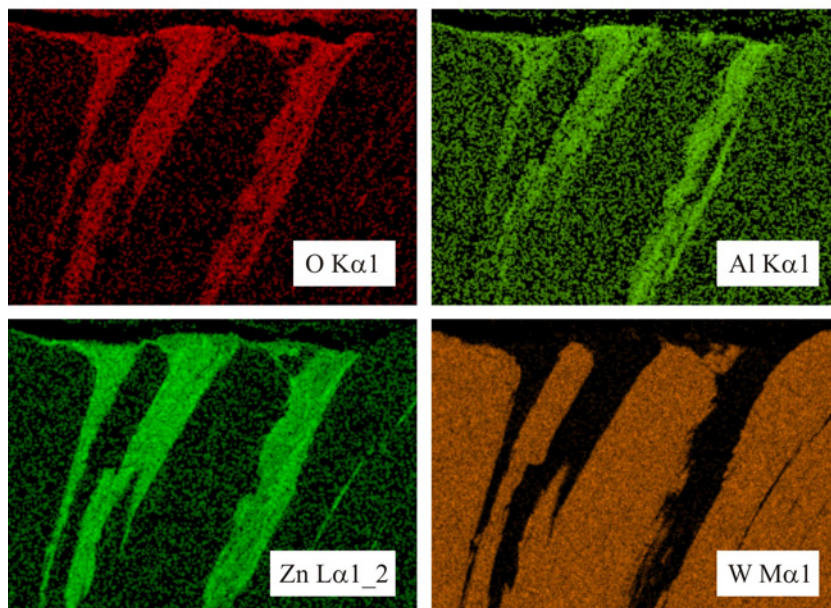
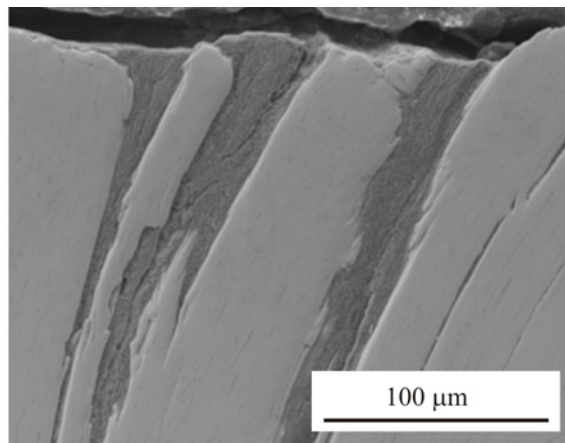


Fig. 10. Detailed EDS maps of the cross-section of the tungsten insert in compound electrode tip after 800 welds.

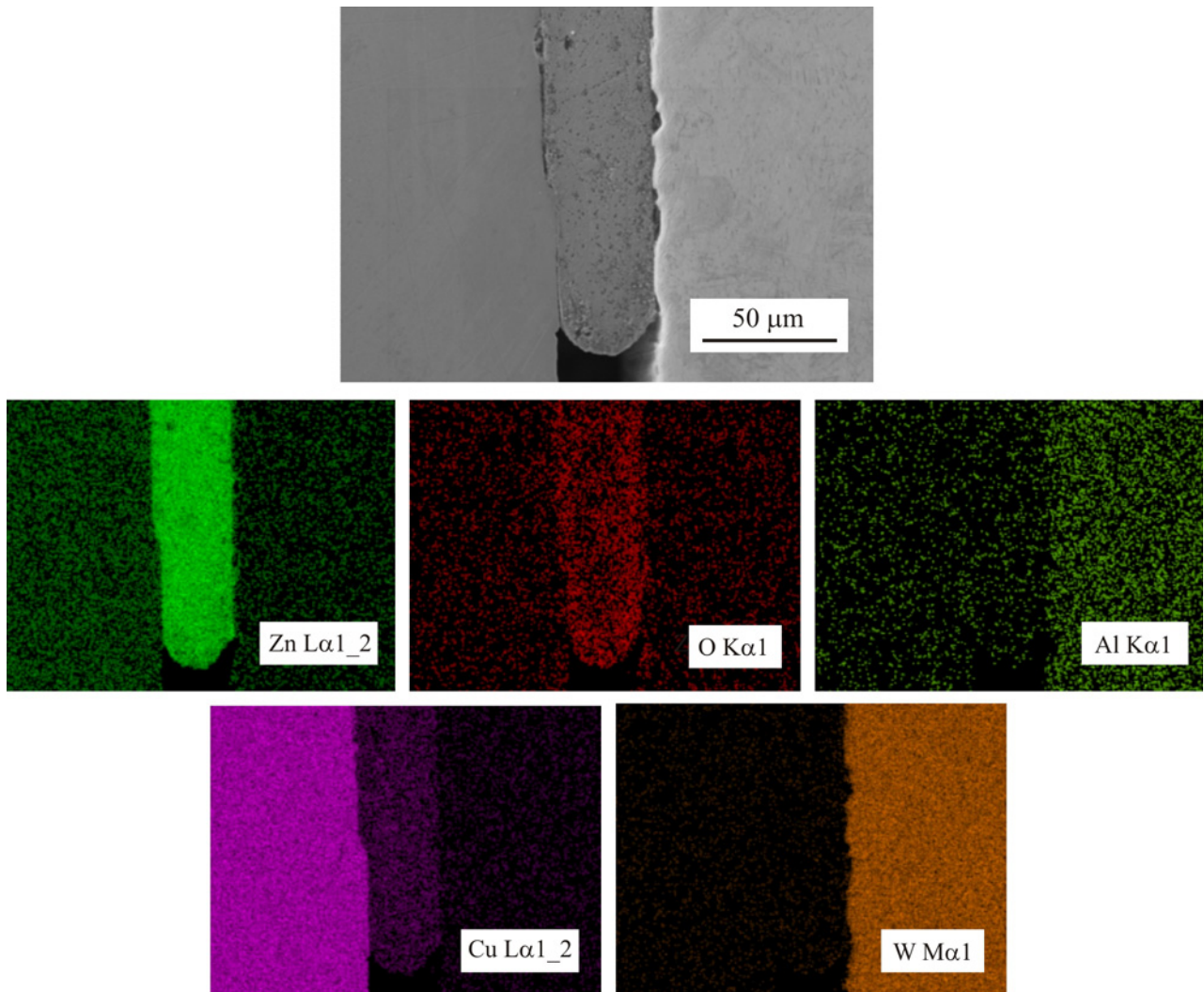


Fig. 11. Detailed EDS maps of the cross-section of the tungsten insert in the volume of the compound electrode after 800 welds (interface between insert and matrix at the end of new continuous phase).

is predominantly found deeper in the cracks. This is also confirmed by the detailed map analysis of the end of the continuous phase at the matrix-insert interface (Fig. 11).

The concave-shaped end of the infiltrated continuous phase from the surface indicates that this Zn-based phase is wetted neither with the CuCrZr matrix nor with the tungsten. Further observations have shown that this phase does not react with tungsten insert at all. In the case of CuCrZr matrix, the adjacent area seems to be only slightly influenced by diffusion processes due to thermal stress during 800 welds. Line analysis of the elements near the end of the continuous phase interface confirms that the diffusion processes took place between the continuous phase and the CuCrZr matrix (Fig. 12).

4. Conclusions

The microstructure of the tungsten insert in CuCrZr compound electrode after 800 welds using resistance spot welding of galvanized sheets HX 220 BD-Z100 MBO 0.8 mm thick protective coating was investigated. For comparison, the microstructure of the tungsten insert in CuCrZr compound electrode after 800 cycles of mechanical loading against the same material at room temperature with an applied force up to $F = 2.2$ kN (the identical conditions as for welding) was also investigated.

At room temperature, the cracks in the tungsten insert were observed. They are mostly due to the presence of tungsten oxides originating from the technology of tungsten rods production (adhesive joints in wolfram bulk).

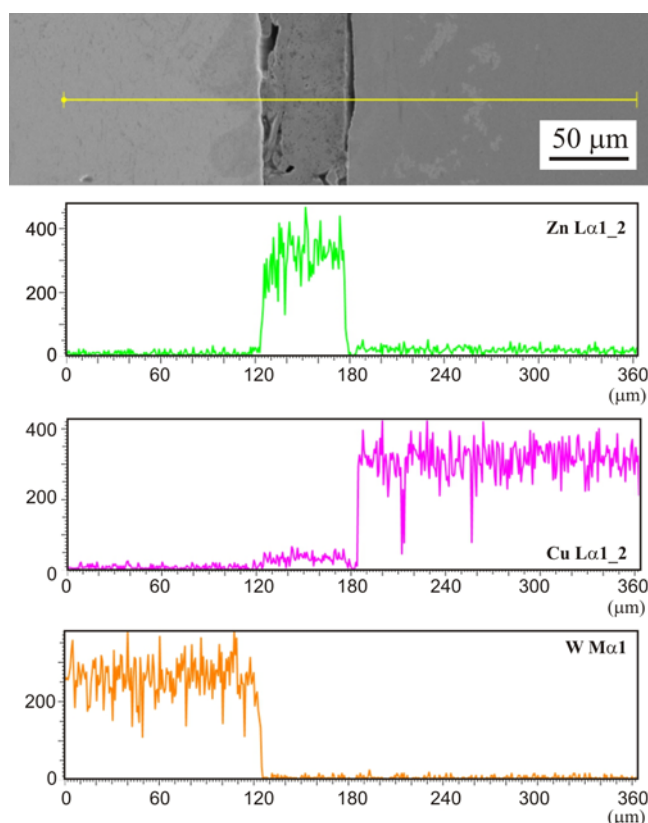


Fig. 12. EDS line analysis of the cross-section of the volume of the compound electrode after 800 welds (interface between insert and matrix near the end of a new continuous phase).

The microstructural results confirmed that Zn did not dissolve in tungsten. From this point of view, tungsten can be considered as a suitable material for compound electrode core inserts for resistance spot welding of galvanized steel sheets.

However, a new phenomenon, which negatively influences the life of the compound electrode tip, has emerged from microstructural observations. The Al was found on the surface of the tungsten insert. The presence of aluminium is most likely in the form of aluminium oxides, and also the presence of Al-tungsten phases (WAl₄ created at 1326 °C and WAl₅ created at 870 °C) is not fully excluded.

These aluminium oxides/phases have a significant effect on the interface resistivity thus increasing the temperature at the interface of the compound electrode and the welded steel sheets. The rise of temperature also affects the deformation of the electrode tip during welding.

Therefore, the significant number of cracks on the tungsten insert is most likely to be associated with the combined heat and mechanical strain on the compound electrode and due to the presence of tungsten oxides originating from the technology of tungsten rods production (adhesive joints).

The presence of Al or alumina on the tungsten insert also affected welding process (above 200 welds and more): the partial stamping of the compound electrode to the welded material was observed.

An important result is that it is necessary to address this problem, which, as was shown, affects the life of the studied compound electrode with tungsten insert. One possibility is to use tungsten insert not prepared via usual commercial technique (cold pressing of tungsten powder followed by hot rotating forging and subsequent drawing to the desired rod size), but by directly pressing and sintering to net shape of the insert. In this case, adhesive joints with tungsten oxides can be avoided thus decreasing the probability of the insert cracking at all.

Acknowledgements

Slovak Grant Agency grant VEGA 1/0385/15 and SRDA Agency grant APVV SK-PL-2015-0003 financial supports are gratefully acknowledged.

References

- [1] Hu, X., Zou, G., Dong, S. J., Lee, M. Y., Jung, J. P., Zhou, Y.: *Materials Transactions*, 51, 2010, p. 2236. [doi:10.2320/matertrans.M2010239](https://doi.org/10.2320/matertrans.M2010239)
- [2] Zou, J., Zhao, Q., Chen, Z.: *Journal of Materials Processing Tech.*, 209, 2009, p. 4141. [doi:10.1016/j.jimatprotec.2008.10.005](https://doi.org/10.1016/j.jimatprotec.2008.10.005)
- [3] Parker, J. D., Williams, N. T., Holliday, R. J.: *Sci. and Tech. of Welding and Joining*, 3, 1998, p. 65. [doi:10.1179/136217198791153204](https://doi.org/10.1179/136217198791153204)
- [4] De Dorn, A. L., Gupta, O. P.: *Science and Technology of Welding and Joining*, 5, 2000, p. 49. [doi:10.1179/stw.2000.5.1.49](https://doi.org/10.1179/stw.2000.5.1.49)
- [5] Saito, T., Miyazaki, Y., Sakaiyama, T., Takahashi, Y., Mizuhashi, N.: *Nippon Steel Technical Report No. 65*, 1995, p. 25.
- [6] Kováčik, J., Baksa, P., Emmer, Š.: *Acta Metallurgica Slovaca*, 22, 2016, p. 52. [doi:10.12776/ams.v22i1.628](https://doi.org/10.12776/ams.v22i1.628)
- [7] Dong, S., Zhou, N.: *China Mech. Eng.*, 19, 2008, p. 2236.
- [8] Rajkovic, V., Bozic, D., Jovanovic, M. T.: *Materials and Design*, 31, 2010, p. 1962. [doi:10.1016/j.matdes.2009.10.037](https://doi.org/10.1016/j.matdes.2009.10.037)
- [9] Emmer, Š., Baksa, P., Kováčik, J.: *Kovove Mater.*, 53, 2015, p. 423. [doi:10.4149/km-2015_6_423](https://doi.org/10.4149/km-2015_6_423)
- [10] Bergqvist, L.: *Technical Report 4/2011 – Copper Zirconium alloys*. Vällingby, Lesjöfors AB 2012.
- [11] Kurtz, W., Vanecek, H.: *Gmelin Handbook of Inorganic and Organometallic Chemistry*. 8th Edition. Berlin Springer Science & Business Media 2013. ISBN3662086905
- [12] Votava, J.: *Acta Technologica Agriculturae*, 17, 2014, p. 49. [doi:10.2478/ata-2014-0011](https://doi.org/10.2478/ata-2014-0011)